Dual porosity system analysis of the Japan Plate Boundary Thrust that generated the 2011 Sendai Tsunami.

F. Cappuccio[1], M. Kirilova[1], V. Toy[1], S.Mills[2], K. Gessner[3]

[1]DEPARTMENT OF GEOLOGY, UNIVERSITY OF OTAGO, P.O. BOX 56, DUNEDIN 9054, NEW ZEALAND

[2]DEPARTMENT OF COMPUTER SCIENCE, UNIVERSITY OF OTAGO, P.O. BOX 56, DUNEDIN 9054, NEW ZEALAND

[3]GEOLOGICAL SURVEY OF WESTERN AUSTRALIA, DEPARTMENT OF MINES, INDUSTRY REGULATION AND SAFETY, 100 PLAIN STREET EAST, PERTH, WA, 6004, AUSTRALIA

INTRODUCTION

The Pacific Plate subducts beneath the Japan Plate at rate of ~79-92mm/yr. Along this slip zone the Tohoku-Oki earthquake (MW = 9.0-9.1) occurred on 11 March 2011, generating the Sendai Tsunami. The hypocenter was ~ 70 km ESE of the Oshika Peninsula of Tohoku and at an underwater depth of approximately ~ 29 km.

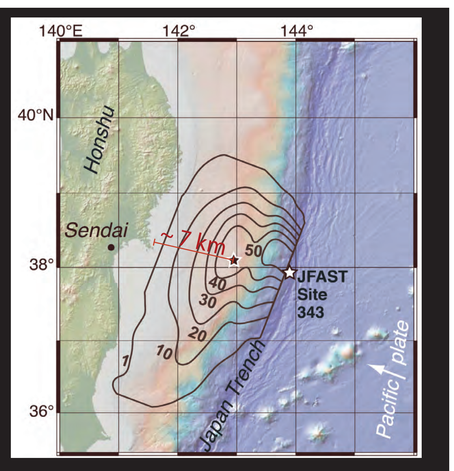

Only 13 months after the earthquake, the Japan Trench Fast Drilling Project (JFAST) collected well log and core data around the slip zone at drill site C0019. The borehole, which extended 850mbsf deep, sampled the decollement (the contact between deformed bedding of the overlying prism and flat-lying basal sediments of the subducting plate) at ~ 820mbsf.

We have studied the 1.0m length of core '17R' that sampled part of the <5.0m thick decollement (Chester et al., 2013, Kirkpatrick et al., 2015). Because shallow slow earthquakes have been reported from the Japan Trench subduction zone (offshore Miyagi), the descriptions provide a framework that may allow diagnosis of the potential of other faults to accommodate not only coseismic slip but also slow slip events.

The samples are particularly rich in smectite compared to other fault principal slip zones worldwide. These clays are arranged in a phaccoidal compaction fabric, which comprises lenticular lozenges of aligned clays bounded by anastomosing dark seams (Toy et al., 2018). The resultant fabric is an interlinked weak layer morphology similar to those that elsewhere are inferred to accommodate aseismic creep. However, the strong alignment of these clay minerals imparts low cross-fault permeability which could facilitate dynamic weakening by fluid pressurization if earthquake ruptures do propagate into these materials.

We have examined the geometrical arrangement of intragranular pores and microfractures within these samples from synchrotron micro- and nano-CT scans, to determine the relative roles these two types of structures play in storage and transportation of fluids, that can weak the rock.

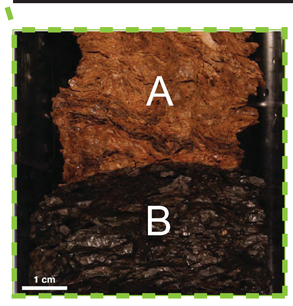

A) Bright reddish-brown scaly smectite-rich clays make up sample 343-C0019E-17R-light
B) Dark brown scaly smectite-rich clays make up sample 343-C0019E-17R-dark

Phacoidal compaction fabric (PCF) in the core "17R" (after Toy et al., 2018)

Anastomosing dark seams and/or aligned clays bound mostly sigmoidal lozenges. Lozenges bounded by shear features (ie. aligned clays) are reasonably denoted as phacoids. Lozenge long axes define a foliation dipping gently with respect to the (vertical) core axis that is disrupted adjacent to later localized structures. The spacing of phacoid-bounding surfaces increases from mm to cm with increasing depth in the core

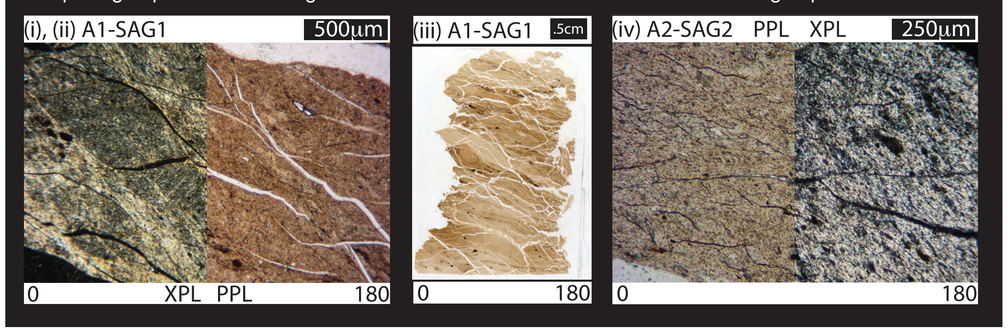

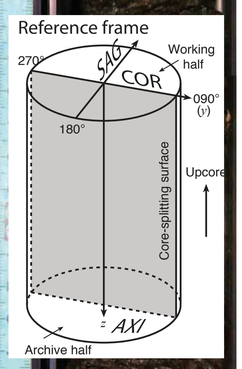

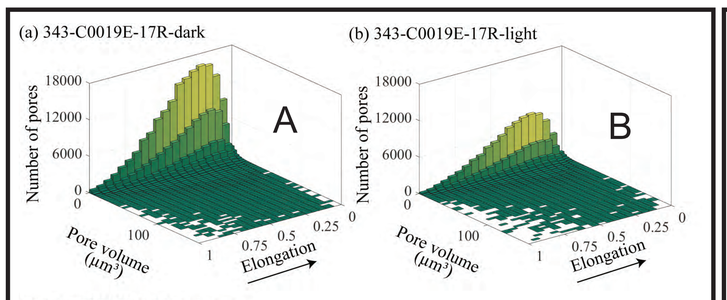

Pores in the JFAST samples (both micro- and nano-sCT) are:
- predominantly ellipsoidal or elongated
- distributed along grain boundaries of the constituent mineral phases

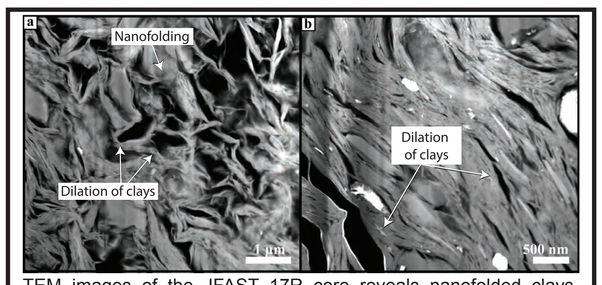

TEM images of the JFAST 17R core reveals nanofolded clays, between which there has been dilation, generating porosity. Pores in this sample are also associated with grain boundaries with different variable sizes. The largest pores are ~ 2 microns in length.

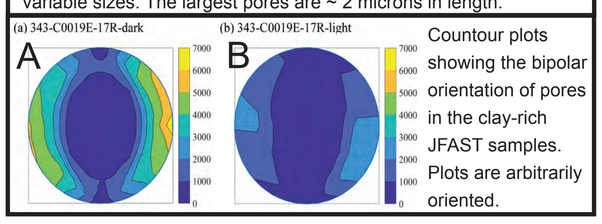

Countour plots showing the bipolar orientation of pores in the clay-rich JFAST samples. Plots are arbitrarily oriented.

Total Porosity (Φ_{TOT}) = 4.38%
Intergrain porosity (Φ_p) = 1.12% (25.6% of the Φ_{TOT})
Fracture porosity (Φ_f) = 3.26% (74.4% of the Φ_{TOT})

Different porosity components were separated in Avizo using a shape parameter threshold, which split blobs from planar objects

Effective porosity (Φ_{eff}) along the three axis:
- X : 1.41 %
- Y : 1.24 %
- Z : 1.47 %

Porosity that is completely connected across the analysed volume parallel to that axis, extracted using a Python script

Physical estimated permeability along the three axis:
- X : 0.25345e-16 m² (0.256814x10⁻⁴ D)
- Y : 3.04380e-16 m² (3.084203x10⁻⁵ D)
- Z : 2.21846e-16 m² (2.247908x10⁻⁵ D)

Estimated with GeoDict software, using Darcy's Law with a set mean flow velocity, fluid viscosity, pressure drop, and media thiickness. Stationary fluid flow is described by the Stokes equation (with LIR solver)

All these plots are for 343-C0019E-17R-light

B

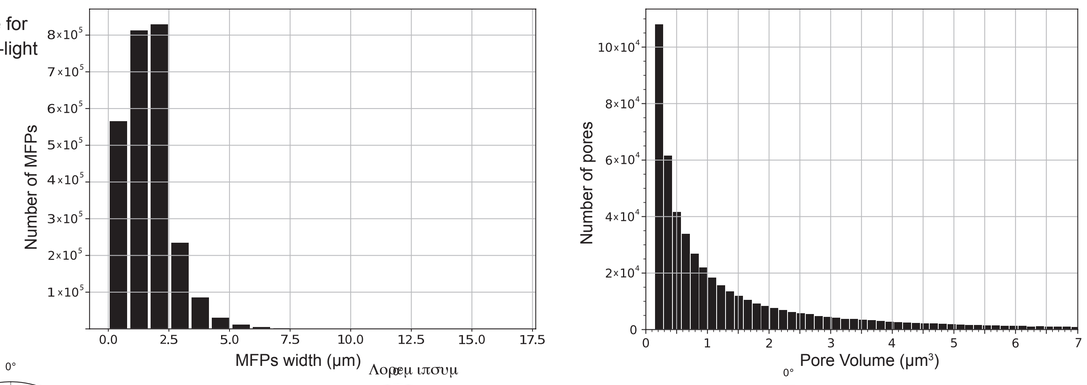

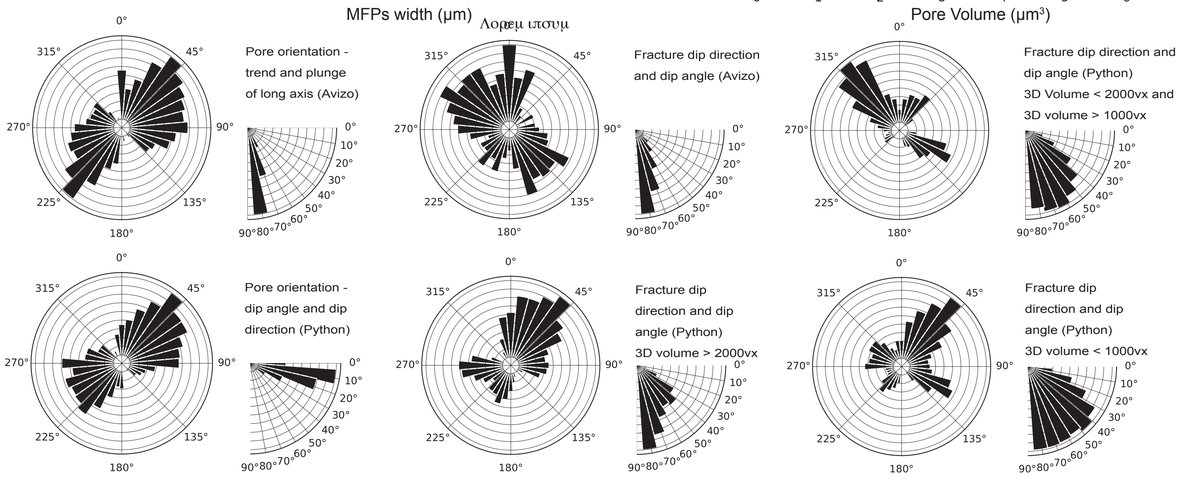

Phi (0, +90) and theta (-180, +180) angles were computed by Avizo using inertia moment. They are defined by the eigenvector of the largest eigenvalue of the covariance matrix.Theta angles are here converted to 0°-360°. The Python code measures the tilt as the angle between the normal of a fitting plane (eigenvector of the smallest eigenvalue of the covariance matrix) and a fixed zenith. The 'orientation' in these plots is the angle between the horizontal projection of the normal vector and an arbitrarily fixed north.

CT-scans were analyzed using commercial software Avizo 9, Matlab, and a Python script. The workflow comprises several steps, summarized here: In Avizo: Pre-processing (filtering, cropping) => Segmentation (of pores and fractures) => Morphological operations (i.e. "connected components") used to exclude cracks => Labels with geometrical characteristics extracted => Further analyses and visualization using Matlab => Separation of pores from fractures based on aspect ratio => Python script measures three-dimensional fracture width and orientation of each voxel lying on the fracture trace

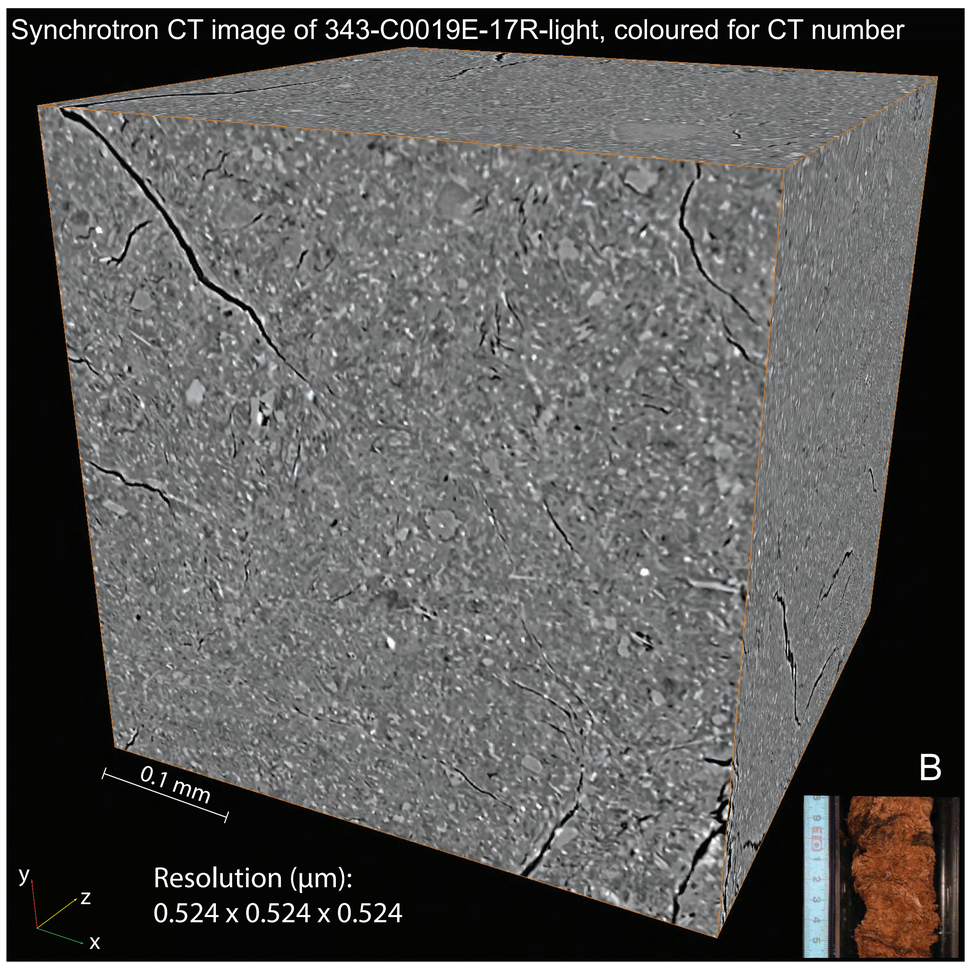

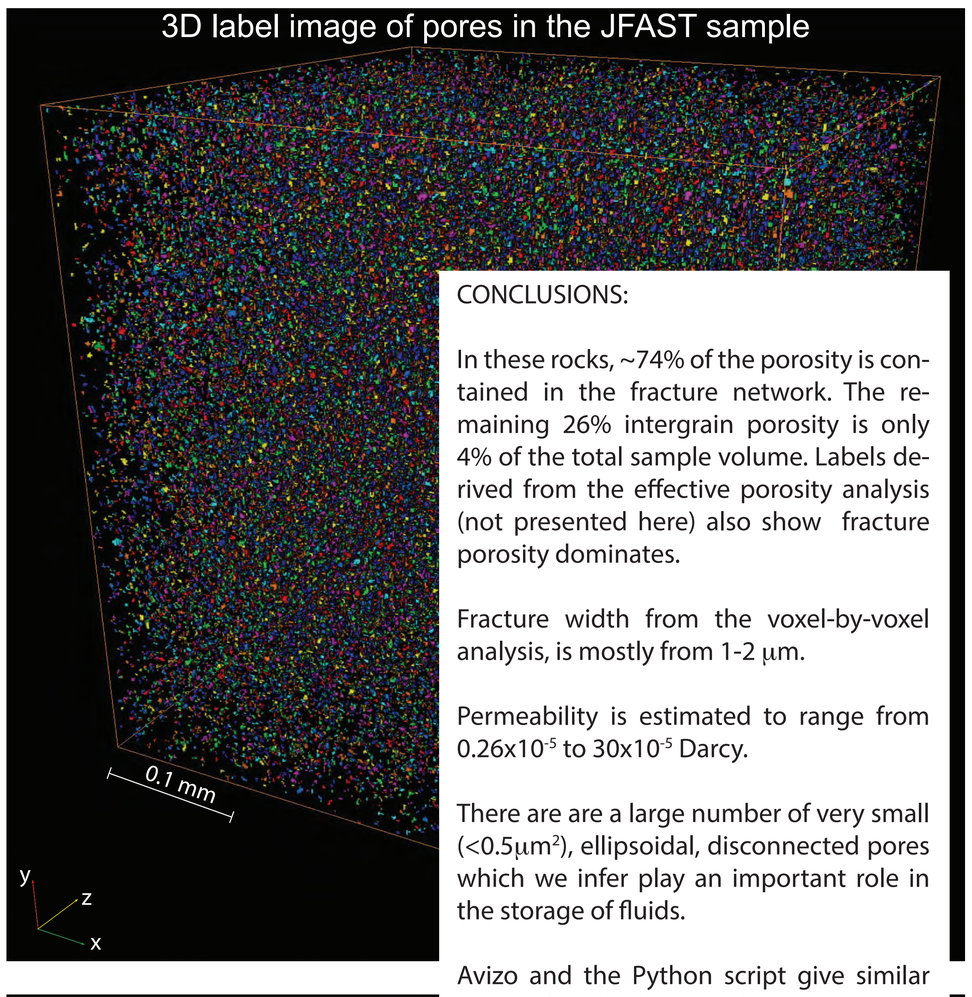

CONCLUSIONS:

In these rocks, ~74% of the porosity is contained in the fracture network. The remaining 26% intergrain porosity is only 4% of the total sample volume. Labels derived from the effective porosity analysis (not presented here) also show fracture porosity dominates.

Fracture width from the voxel-by-voxel analysis, is mostly from 1-2 µm.

Permeability is estimated to range from $0.26x10^{-5}$ to $30x10^{-5}$ Darcy.

There are are a large number of very small (<0.5µm²), ellipsoidal, disconnected pores which we infer play an important role in the storage of fluids.

Avizo and the Python script give similar orientation distributions for pores, but the range of trends is larger from Avizo.

In an arbitrary X-Y-Z reference frame linked only to the CT scans:
- Pores characteristically have bi-polar orientation distributions, with long axes trending at angles of ~50 - 260° to 'X'
- Dominant fractures strike 040-045°,

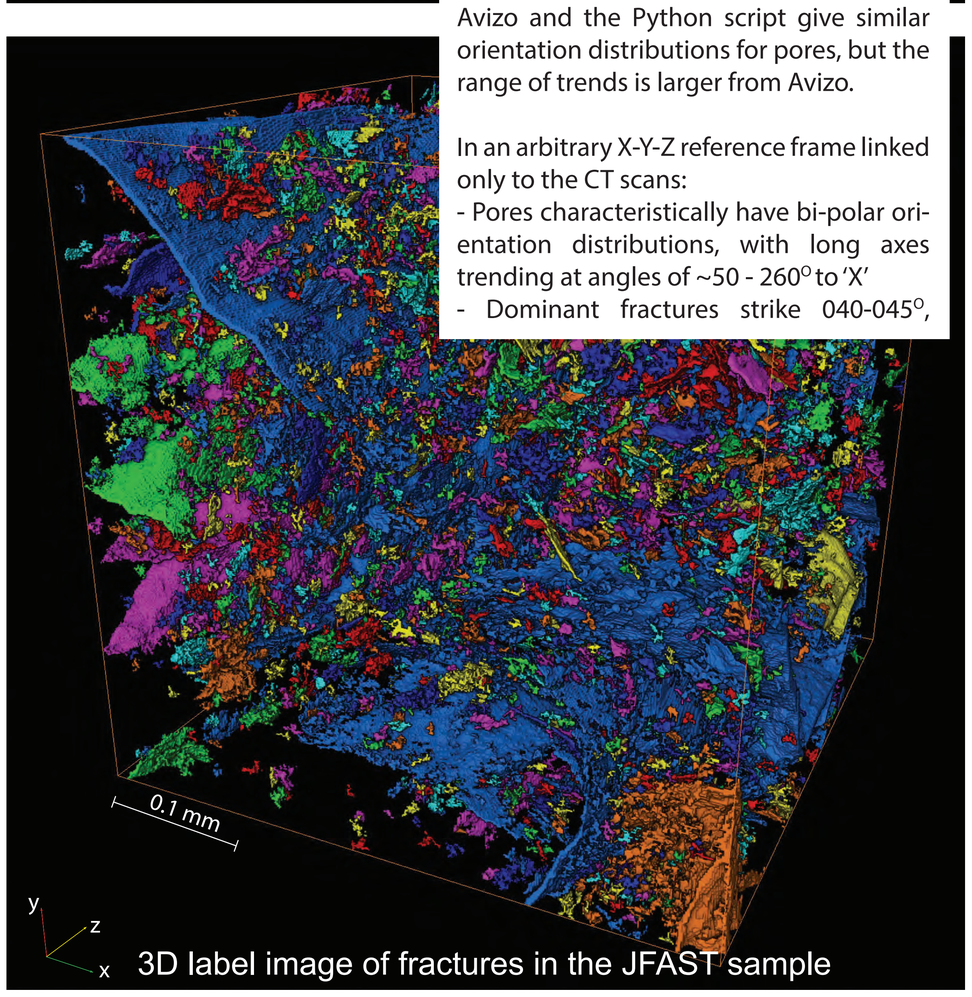

References:
Chester, F.M., Rowe,, C., Ujiie, K., Kirkpatrick, J., Regalla, C., Remitti, F., Moore, J.C., Toy, V.G., Wolfson-Schwher, M., Bose, S., Kameda, J., Mori, J.J., Brodsky, E.E., Eguchi, N., Toczko, S., Expedition 343 and 343T Scientists. 2013. Structure and composition of the plate-boundary slip-zone for the 2011 Tohoku-oki earthquake. Science 342, 1208-1212, doi: 10.1126/1243719 .
Kirkpatrick, J.D., Rowe, C.D., Ujiie, K., Moore, J.C., Regalla, C., Remitti, F., Toy, V.G., Wolfson-Schwehr, M., Kameda, J., Bose, S., Chester, F.M. 2014. Structure and lithology of the Japan Trench subduction plate boundary fault. Tectonics 34(1), 53-69. doi: 10.1002/2014TC003695.
Toy, V.G., Rowe, C., Kirkpatrick, J., Remitti, F., Wolfson-Schwehr. M., Ujiie, K., Tulley, C. 2018. Insights from microstructures of the plate boundary thrust sampled during JFAST into the development of rock fabrics capable of accommodating both slow creep and seismic slip. Abstract and poster presentation at the Gordon Research Conference on Rock Deformation, New Hampshire, USA.